Absolute Cherenkov photon measurements via angular calibration of a fused silica scatter screen

Contact: jesel.patel@stfc.ac.uk

J. K. Patel, D. Neely, C. D. Armstrong, Y. Katzir, A. Dasgupta, D. Treverrow, S. Hawkes
Central Laser Facility, STFC, OX11 0QX, United Kingdom

E. Zemaityte, R. Gray, A. Horne, T. Frazier, P. McKenna
University of Strathclyde, G4 0NG, United Kingdom

S. Rozario, J. Wood, M. Backhouse
Imperial College London, SW7 2BU, United Kingdom

R. Deas, H. Thomas, J. Wilkinson, S. Dorkings, R. Giordmaina, P. Dodd, J. May
Dstl, Fort Halstead, TN14 7BS, United Kingdom

1 Introduction

Cherenkov radiation is the electromagnetic emission (typically of visible to ultraviolet wavelength) produced when a charged particle travels faster than the speed of light in a medium with refractive index > 1. Imaging of Cherenkov radiation can be used to diagnose the charge of high energy electron bunches, such as those produced in laser-plasma interactions [1–3]. In a recent experiment using the Astra-Gemini laser target area 3 (hence referred to as 'Gemini TA3'), a fused silica block with a ground surface acting as a scatter screen was used to image the forward beam of Cherenkov radiation produced by such high energy electrons, using cooled Andor NEO scientific CMOS cameras [4]. An expected light yield in photons can be derived from Cherenkov theory, which can be used to verify experimental results, if an absolute calibration of the scatter screen is carried out using the same linear CMOS camera [5, 6]. The results and methods of such a calibration are reported here, for the benefit of past and future work done using this method.

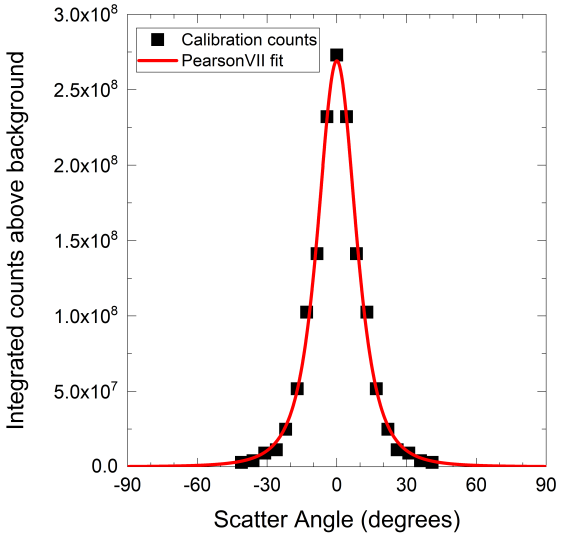

Figure 1: PearsonVII fit of scatter screen calibration data. Values of $m = 1.88$ and $w = 9.32$ are obtained (see Eq (3)).

2 Scatter screen calibration

To obtain the number of Cherenkov photons incident to the scatter screen for measurements at different angles, a laser of known power is directed to the scatter screen. A 1 mW, 532 nm laser was directed through the fused silica as shown in Fig. 2, and 0.1 sec exposures of the scattered light were imaged using the CMOS camera. The number of photons incident to the scatter screen is given by the laser power, P, wavelength, λ, and exposure time, t,

$$N_\gamma = \frac{Pt\lambda}{hc}, \tag{1}$$

where h is Planck's constant, and c is the speed of light. In practice, the laser was passed through ND filters with optical density, d, and a plastic window coupled to the fused silica using optical coupling gel. As a result, the real number of photons incident to the scatter screen is

$$N_\gamma = \frac{Pt\lambda}{hc} \times 10^{-d} \times T, \tag{2}$$

where T is the transmission of the plastic window – fused silica boundary. We assume that $T = 0.8$ here. Taking exposures at various angles to normal, and obtaining the integrated counts of the imaged laser spot produces an angular distribution of the scattered flux, as shown in Fig. 1. Fitting to this data gives the number of counts expected to be measured at the Gemini TA3 cameras' angular position to the scatter screen. The expression found to achieve the best fit is the Pearson VII, which is essentially a Lorentzian raised to a power, m, which adds a degree of freedom to the shape of the fit. The

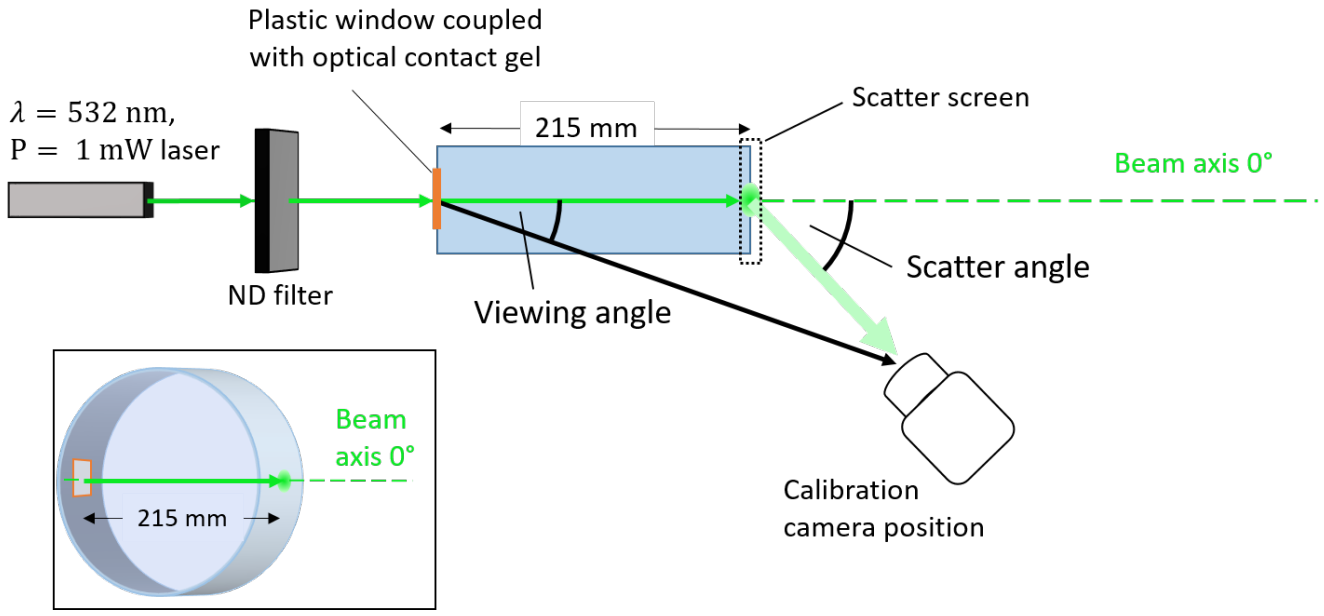

Figure 2: Top-view schematic of scatter screen calibration set up. Inset (bottom-left) is side-view illustration of fused silica block and scatter surface.

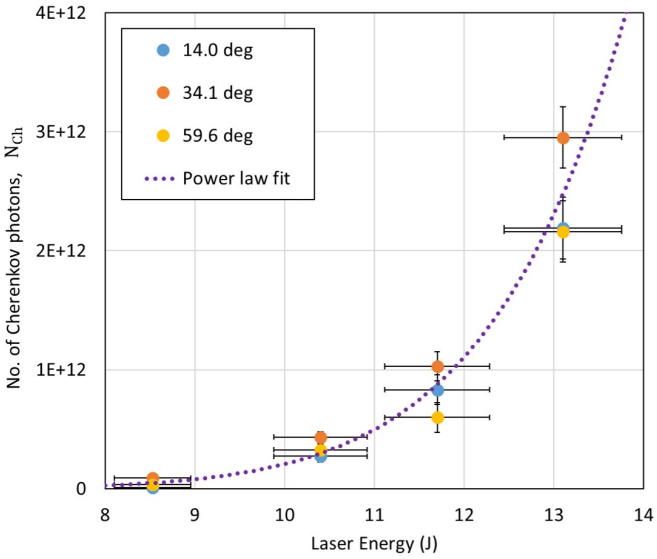

Figure 3: Number of Cherenkov photons, N_{Ch}, with laser energy at three scatter angles. Dotted line is a power law fit of the data averaged over the three scatter angles.

distribution is described by

$$I(\theta) = I_{max} \frac{w^{2m}}{[w^2 + (2^{1/m} - 1)(\theta - \theta_0)]^m}, \quad (3)$$

where I_{max} is the peak number of counts, w is the half width at half maximum, and θ and θ_0 are the scattering angle and scattering angle at maximum counts, respectively. Notably, Eq (3) tends towards a Lorentzian as $m \longrightarrow 1$, and a Gaussian when $m \gg 1$, i.e. $m \gtrsim 10$. The obtained value, $m = 1.88$ (2 s. f.) indicates that the angular flux distribution of the scatter screen used is more closely described as Lorentzian than as a Gaussian, with more significant contributions from its 'tails'.

Approximating the change in counts at different distances to the scatter screen using the inverse-square law, we obtain the number of counts at the distances used in the Gemini TA3 experiment. The ratio of the number of photons, N_γ, to the number of counts calculated from the calibration measurements, N_{counts}, is then applied to the integrated counts of the images of the Cherenkov photons on the scatter screen to obtain an approximate number of Cherenkov photons, N_{Ch};

$$N_{Ch} = N_\gamma / N_{counts}. \quad (4)$$

The number of Cherenkov photons obtained at the scatter imaging angles, 14.0°, 34.1° and 49.6°, (corresponding to Gemini TA3 'viewing angles' 10°, 25° and 40°, respectively), and four Gemini laser energies are plotted in Fig. 3. The calculated number of photons at the three imaging angles agree relatively well, indicating the validity of the calibration technique for obtaining an approximate number of photons.

3 Comments

A method for calibrating a Cherenkov radiator and scatter screen has been demonstrated to produce consistent results for measurements obtained at three different angular positions. The number of Cherenkov photons which were produced in the Gemini TA3 experiment at various laser energies appear to agree with preliminary theoretical estimates ($\sim 10^{12}$ photons), though a rigorous calculation is not presented here. To further develop this calibration technique, measurements of the surface roughness of the scatter screens are required, and a more considered evaluation of the scattering behaviour of Cherenkov light compared with the green (532 nm) laser should be undertaken, accounting for the impact of the spectral difference on the calibration method. With development, there is promise for a Cherenkov based electron beam diagnostic, especially in high repetition rate laser-plasma interaction environments.

References

[1] Liu, H., Liao, G-Q., Zhang, Y-H. et al., 2018, *Cherenkov radiation-based optical fibre diagnostics of fast electrons generated in intense laser-plasma interactions* Review of Scientific Instruments **89**, 083302 (2018)

[2] Adli, E. et al., 2015 *Cherenkov light-based beam profiling for ultrarelativistic electron beams*Nucl. Instrum. Methods Phys. Res., Sect. A **783**, 35-42 (2015)

[3] Blumenfeld, I., Clayton, C., Decker, F. et al. *Energy doubling of 42 GeV electrons in a metre-scale plasma wakefield accelerator* Nature **445**, 741–744 (2007)

[4] Andor Neo 5.5 sCMOS Specifications `https://andor.oxinst.com/assets/uploads/products/andor/documents/Neo-sCMOS-Specifications.pdf` Oxford Instruments (accessed January 2020)

[5] Dasgupta, A., Armstrong, C. D., Neely, D., Rusby, D., Scott, G. *Assessment of cameras for low intensity acquisitions* Central Laser Facility (2019)

[6] Rusby, D., *Study of Electron Dynamics and Applications from High-Power Laser-Plasma Interactions* PhD Thesis, University of Strathclyde (2017)

Appendix

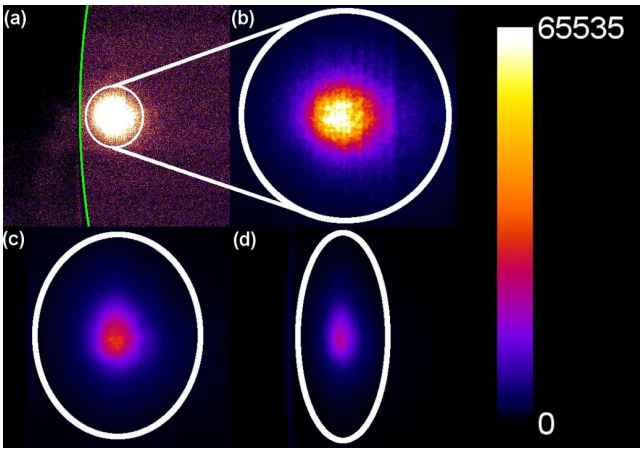

Figure 4: Sample calibration images: (a) at 10° scaled for high contrast, showing the edge of the fused silica radiator (green line) and illustrating how the region of interest (ROI) was selected for sampling; (b) at 10°, magnified to ROI and in linear scaling across entire camera dynamic range; (c) at 25°; and (d) at 40°. (c) and (d) are presented with similar magnification and the same scaling as (b).